Hindawi Publishing Corporation
International Journal of Photoenergy
Volume 2010, Article ID 902385, 9 pages
doi:10.1155/2010/902385

Research Article

Preparation of a Counter Electrode with *P*-Type NiO and Its Applications in Dye-Sensitized Solar Cell

Chuen-Shii Chou,[1,2] Chin-Min Hsiung,[1,2] Chun-Po Wang,[2] Ru-Yuan Yang,[1,3] and Ming-Geng Guo[2]

[1] *Research Center of Solar Photo-Electricity Applications, National Pingtung University of Science and Technology, Pingtung 912, Taiwan*
[2] *Powder Technology R&D Laboratory, Department of Mechanical Engineering, National Pingtung University of Science and Technology, Pingtung 912, Taiwan*
[3] *Department of Materials Engineering, National Pingtung University of Science and Technology, Pingtung 912, Taiwan*

Correspondence should be addressed to Chuen-Shii Chou, cschou@mail.npust.edu.tw

Received 30 November 2009; Revised 20 March 2010; Accepted 10 May 2010

Academic Editor: Stephen M. Goodnick

This study investigates the applicability of a counter electrode with a *P*-type semiconductor oxide (such as NiO) on a dye-sensitized solar cell (DSSC). The counter electrode is fabricated by depositing an NiO film on top of a Pt film, which has been deposited on a Fluorine-doped tin oxide (FTO) glass using an ion-sputtering coater (or E-beam evaporator), using a simple spin coating method. This study also examines the effect of the average thickness of TiO_2 film deposited on a working electrode upon the power conversion efficiency of a DSSC. This study shows that the power conversion efficiency of a DSSC with a Pt(E)/NiO counter electrode (4.28%) substantially exceeds that of a conventional DSSC with a Pt(E) counter electrode (3.16%) on which a Pt film was deposited using an E-beam evaporator. This result is attributed to the fact that the NiO film coated on the Pt(E) counter electrode improves the electrocatalytic activity of the counter electrode.

1. Introduction

Solar power is the most notable among renewable energy resources because of its low environmental impact and global availability. Among alternative forms of solar cells, dye-sensitized solar cells (DSSCs), as proposed by O'Regan and Grätzel [1], have attracted considerable interest since 1991 because of its properties, such as low production cost and low environmental impact during fabrication [2, 3].

In the past few years (2006–2009), several methods have been utilized in modifying the structure of a working electrode (TiO_2 electrode) to improve the performance of DSSCs [4–22]. Novel sensitizers were synthesized and applied in DSSCs to promote the absorption of the visible spectrum [3, 23–29]. Novel electrolytes were proposed to prevent leakage of the electrolyte or to increase the lifetime (or performance) of DSSCs [30–35]. Moreover, a quasisolid DSSC with straight ion paths based on an anodically oxidized Al_2O_3 film, which was full of nanopores from one side of the film to the other, was presented [36].

The counter electrode is an equally important component of the DSSC. The role of the counter electrode is to transfer electrons from an external circuit to the tri-iodide and iodine in the redox electrolyte. Currently, a layer of platinum (Pt) coated on a transparent conducting oxide (TCO) substrate is widely used as a counter electrode in DSSCs. Besides platinum (Pt), carbon materials (such as graphite powder and carbon black [37, 38], hard carbon spherule [39], single-walled carbon nanotubes [40], multiwalled carbon nanotubes [41], and nanosized carbon powder [42, 43]) have been used to prepare platinum-free counter electrodes.

Aside from the carbon materials, counter electrodes with metal oxide biphase materials (such as Pt/NiO [44, 45] and Pt/TiO_2 [45]) have been prepared using an RF magnetron cosputtering system. However, these highly efficient Pt/NiO (or Pt/TiO_2) bi-phase counter electrodes are

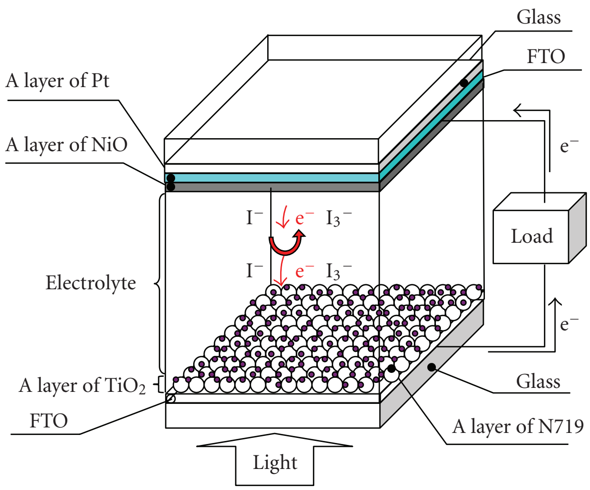

Figure 1: Schematic of the dye-sensitized solar cell with a Pt/NiO counter electrode.

obtained using an expensive vacuum technology which requires a sophisticated process control. Aside from this observation, Kay and Grätzel reported that a small amount of platinum might be dissolved in the electrolyte by oxidation and complex formation with iodide/tri-iodide (such as PtI_4 or H_2PtI_6) [37]. This may degrade the performance of counter electrodes after a certain period of exposure to light. Accordingly, decreasing the oxidation of Pt film in contact with the electrolyte is one of the most important factors in increasing the power conversion efficiency of DSSC; this is worthy of further study.

Therefore, in this study, a simple method (i.e., spin coating) was used to deposit a NiO film on top of a Pt film (Figure 1), which had been deposited on a FTO-glass (Fluorine-doped tin oxide, SnO_2:F) substrate using an E-beam evaporator (or ion-sputter coater) to protect the Pt film from oxidation and corrosion. The effect of *P*-type NiO on the electrocatalytic activity of the counter electrode and the power conversion efficiency of DSSC was investigated. A comparison of a DSSC with the proposed counter electrode with the conventional DSSC was also made in this study.

2. Experimental Details

The experiments involved (1) preparing the colloid of TiO_2 particles (P-25); (2) preparing the working electrode and measuring its properties; (3) preparing the colloid of *P*-type NiO; (4) preparing the counter electrode and measuring its properties; (4) assembling the DSSC by fitting the working electrode, the counter electrode, the electrolyte, and the copper conductive tape; (5) making J-V measurements of the DSSC.

2.1. Preparing and Measuring the Working Electrode. Fabricating a DSSC working electrode with a film of TiO_2 particles (Figure 1) followed these steps: (1) a colloid of TiO_2 particles (P-25) was prepared and homogenized; (2) using spin coating, the colloid of TiO_2 particles was deposited on top of a FTO-glass substrate, and it was then sintered at 500° C for 1 h in a high-temperature furnace (Thermolyne, 46100); (3) the FTO-glass substrate with the film of TiO_2 particles was immersed into a (3×10^{-4} M) solution of N-719 dye (Ruthenium, $RuL_2(NCS)_2$) and ethyl alcohol (CH_3CH_2OH, 95%) at 70°C for 6 h. The area of TiO_2 electrode of DSSC was 0.25 cm^2 in this study.

An α-step (Dekeak 6M) surface profiler was utilized to obtain the average thickness of the film on the FTO-glass substrate of the working electrode. In order to show the crystal structure of the TiO_2 powder, which was obtained by heating the solution of $TiCl_4$, its X-ray diffraction (XRD) patterns were measured using a powder X-ray diffractometer (Shimadzu, XRD-6000).

2.2. Preparing and Measuring the Counter Electrode. The procedure for fabricating a counter electrode of DSSC with a film of Pt sandwiched between a NiO film and a FTO-glass substrate (Figure 1) is as follows. (1) The *P*-type NiO was obtained by annealing the Ni powder in a high-temperature furnace at 500°C; (2) the NiO colloid was prepared by mixing 1 g of NiO with solvents (20 ml of DI water, 1 ml of ethanol, 0.1 ml of acetylacetone, and 0.1 ml of Triton X-100) and then homogenized in an ultrasonic homogenizer for 30 min; (3) using spin coating, 2-3 ml of the NiO colloid was deposited on top of a Pt film, which had been deposited on the FTO-glass substrate using an E-beam evaporator (or ion-sputter coater); (4) this substrate was then sintered at 500°C for 1 h in a high-temperature furnace.

In this study, in order to show the effect of the vacuum level on the performance of a DSSC, an E-beam evaporator (Kaoduen Tech. Corp.) with a vacuum level of 4×10^{-7} Torr and an ion-sputter coater (Hitachi E-1010) with a vacuum level of 10^{-2} Torr were used to deposit a Pt film on the FTO-glass substrate of the counter electrode. The area of a Pt film of counter electrode was 4.0 cm^2 in this study. Aside from this, the two-stage spin coating was used in this study: (1) in the first stage, the rotation speed of 1000 rpm and the duration of 5 s were used to remove the extra NiO colloid from the substrate; (2) in the second stage, the rotation speed of 1500 rpm and the duration of 15 s were used to homogenize the NiO film on the substrate.

The image and the micrograph of the counter electrode with a Pt film were obtained using a digital camera (Panasonic DMC-LZ2) and a scanning electron microscope (HITACHI S-4700), respectively. The reflectance and the cyclic voltammogram (CV) of the counter electrode were obtained using a UV-VIS-NIR spectrophotometer (Jasco V-600) and an electrochemical workstation (CH Instruments CHI-660C), respectively. Further, the surface roughness and the 3D micrograph of the counter electrode were obtained using a atomic force microscope (Digital Instrument NanoMan-NS4+D3100).

2.3. Assembling and Testing the DSSC. The working electrode, the counter electrode, and the copper conductive tape (Ted Pella) were fitted together, with the space between two electrodes adjusted to approximately 25 μm for the liquid

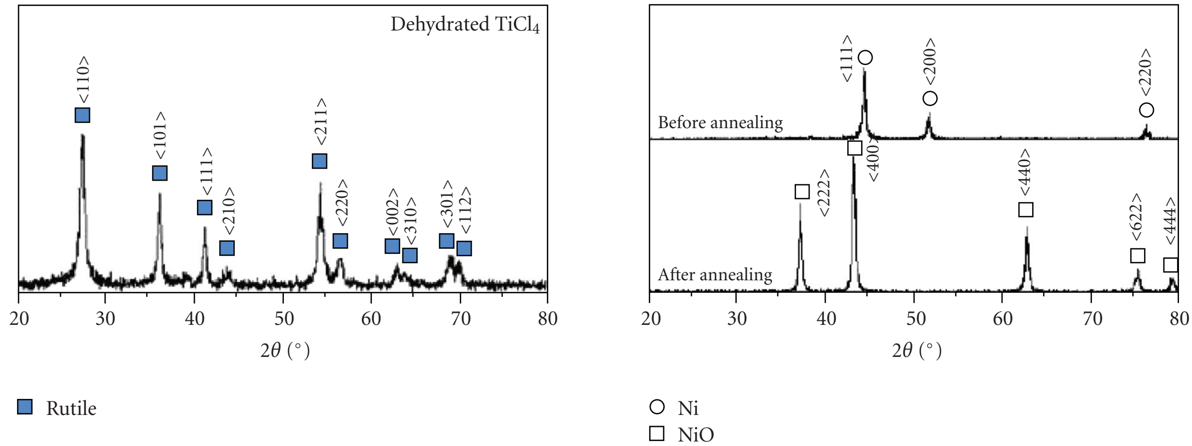

(a) (b)

Figure 2: XRD patterns of Ni, NiO, and dehydrated $TiCl_4$.

electrolyte. After sealing, the liquid electrolyte was injected into the cell through a prepared hole in the cell. The detailed preparation of the photoanode and the DSSC assembly were presented in [22].

A digital source meter (Keithley 2000) measured the open-circuit photovoltage and the short-circuit photocurrent of the DSSC, and a solar simulator (Science Tech. SS150) illuminated the DSSC. The power conversion efficiency η of the DSSC is determined by

$$\eta(\%) = \frac{V_{oc} J_{sc} FF}{P_{in}} \times 100, \quad (1)$$

where V_{oc}, J_{sc}, and P_{in} represent the open-circuit photovoltage, the short-circuit photocurrent per unit area, and the incident light power (100 mW/cm^2), respectively. Aside from this, fill factor (FF) is given by

$$FF = \frac{V_{max} J_{max}}{V_{oc} J_{sc}}, \quad (2)$$

where V_{max} and J_{max} represent the voltage and the current per unit area at the maximum output power point, respectively.

3. Results and Discussion

3.1. Characteristics of $TiCl_4$ and NiO. Figure 2 shows the X-ray diffraction (XRD) patterns of dehydrated $TiCl_4$, as well as powders of Ni and NiO. The solid square, circle, and square in Figure 3 represent rutile, Ni, and NiO, respectively. From JCPDS 89-4920 (rutile), the XRD patterns of the dehydrated $TiCl_4$ show that three major peaks of rutile at $2\theta = 27.47°$, $2\theta = 36.14°$, and $2\theta = 54.31°$ correspond to the diffraction from the <110>, <101>, and <211> planes, respectively. The purpose of immersing a FTO-glass substrate in the $TiCl_4$ solution before depositing the TiO_2 (P-25) colloid is to prevent the FTO-glass substrate from dye (or electrolyte) contamination, which might penetrate through the cavities of the TiO_2 (P-25) film. Ito et al. observed that $TiCl_4$ treatment induced improvements in the adhesion and mechanical strength of a nanocrystalline TiO_2 layer [22].

From JCPDS 89-5881 (nickel oxide), the XRD patterns of the NiO powder, obtained by annealing the Ni powder, show that three major peaks of NiO at $2\theta = 37.3°$, $2\theta = 43.3°$, and $2\theta = 62.9°$ correspond to the diffraction from the <222>, <400>, and <440> planes, respectively. Instead of depositing and annealing Ni to form a NiO deposit on platinum, we have preferred to spin coat a previously formed NiO before sintering. This is because, compared with the Ni powder, NiO powder can be more easily dispersed in the solvent.

3.2. Characteristics of the Counter Electrode. This study used four kinds of counter electrode: (1) a counter electrode with a Pt film deposited on the FTO-glass substrate using an E-beam evaporator (called Pt(E)), (2) a counter electrode with a Pt film deposited on the FTO-glass substrate using an ion-sputter coater (called Pt(S)), (3) a counter electrode prepared by depositing a NiO film on top of Pt(E) (called Pt(E)/NiO), and (4) a counter electrode prepared by depositing a NiO film on top of Pt(S) (called Pt(S)/NiO).

Figure 3 shows the images and the SEM micrographs (20 kx) of the counter electrodes of Pt(E) and Pt(S). Figure 4 shows the variations in reflectance with light wavelength of the Pt(E), Pt(S),t(E)/NiO, and Pt(S)/NiO counter electrodes. For the counter electrodes used in this study, the reflectance increases with an increase in wavelength. For example, for the Pt(E) counter electrode, as the wavelength increases to 800 nm, its reflectance goes up to 50.4% (Figure 4). The light-reflecting character of the Pt film is desirable because it increases the light harvesting efficiency of the sensitizing dye [45, 46]. Aside from this, at a fixed wavelength, the reflectance of the Pt(E) counter electrode substantially exceeds that of the Pt(S) counter electrode. For example, at a fixed wavelength of 800 nm, the reflectance of the counter electrodes of Pt(E) and Pt(S) are 50.4% and 13.4%, respectively. This result is attributed to the fact that the vacuum level of the ion-sputter coater used in this study (10^{-2} Torr) is not higher than that of the E-beam evaporator (4×10^{-7} Torr), so the target (such as Pt) and the residual

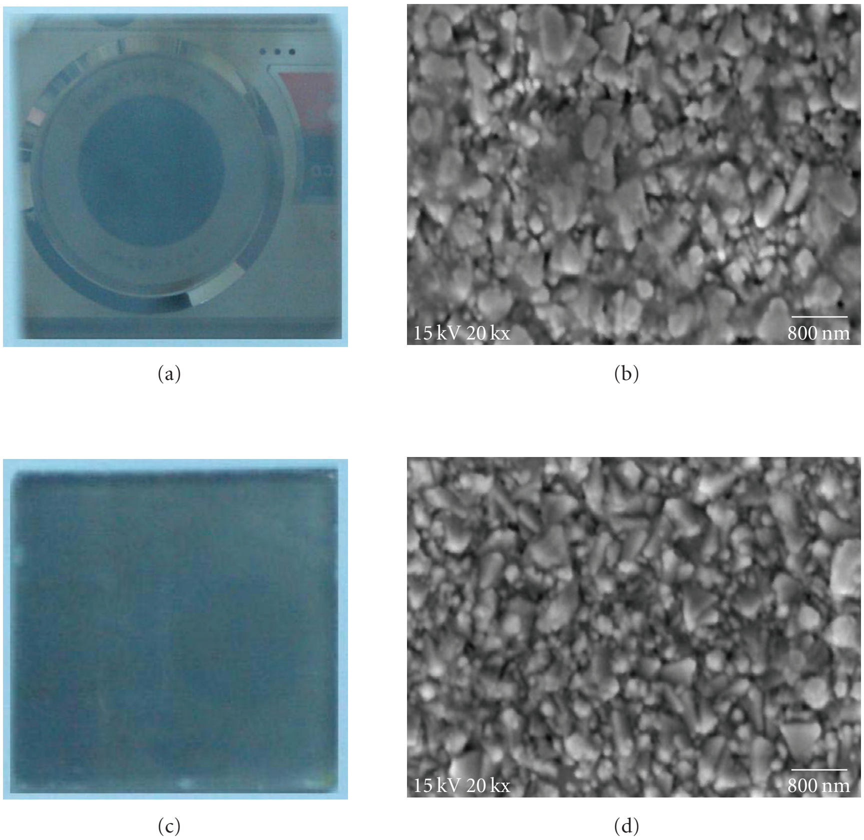

Figure 3: Image of the Pt(E) counter electrode (a), SEM micrograph (20 kx) of the Pt(E) counter electrode (b), image of the Pt(S) counter electrode (c), and SEM micrograph (20 kx) of the Pt(S) counter electrode (d).

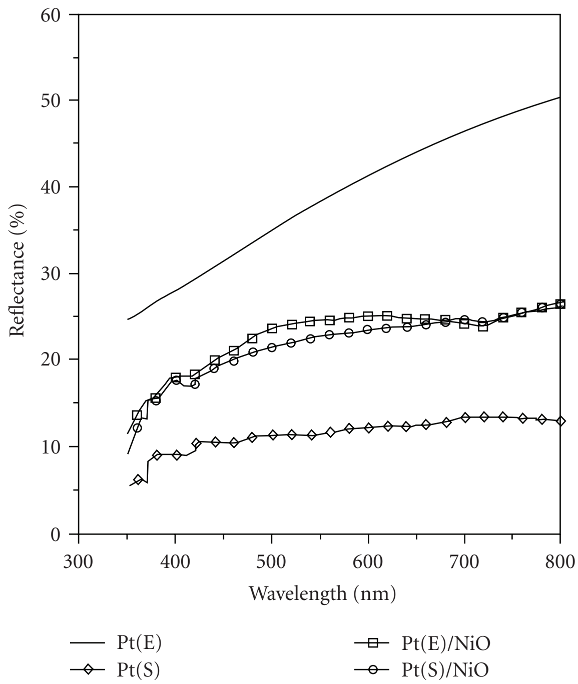

Figure 4: Variations in reflectance with the wavelength of the light for counter electrodes of Pt(E), Pt(S), Pt(E)/NiO, and Pt(S)/NiO.

Table 1: Test conditions and power conversion efficiencies of DSSCs.

	Counter Electrode			Working Elect rode	J_{SC}(mA/cm^2)	V_{OC}	FF(%)	η(%)
		RMS(nm)	Ra(nm)	Average film thickness (μm)				
D1	Pt(E)	18.570	14.213	12.0	9.15	0.65	50.42	3.00
D2				19.0	9.27	0.65	52.49	3.16
D3	Pt(S)	16.734	12.894	11.0	6.11	0.65	58.64	2.33
D4				15.0	8.28	0.65	44.98	2.34
D5	Pt(E)/NiO	123.30	97.321	12.4	9.05	0.65	59.77	3.51
D6				16.0	10.44	0.65	63.15	4.28
D7	Pt(S)/NiO	112.46	92.859	13.1	7.70	0.65	56.40	2.82
D8				14.8	8.45	0.65	50.06	2.92

Note: "(E)", "(S)", RMS, and Ra represent E-beam evaporator, sputtering, root mean square, and roughness average.

substance in the chamber are probably deposited on the substrate during sputtering. Therefore, unlike the Pt(E) counter electrode, the Pt(S) counter electrode is not able to mirror the digital camera, which was used to take images of the counter electrodes (Figure 3). At 800 nm wavelength, the reflectance of the Pt(E)/NiO counter electrode (26.6%) is close to that of the Pt(S)/NiO counter electrode (26.2%). Further, the sheet resistance of the Pt(S) counter electrode (9.73 Ω/sq) also substantially exceeds that of the Pt(E) counter electrode (5.57 Ω/sq).

Figure 5 shows the 3-D microstructures of the Pt(E), Pt(S), Pt(E)/NiO, and Pt(S)/NiO counter electrodes. The surface roughness average (Ra) of the Pt(E) counter electrode (14.213 nm) exceeds that of the Pt(S) counter electrode (12.894 nm), as shown in Figure 5. This is attributed to the fact that compared with evaporation, it is easier to maintain a stable deposition rate during sputtering, and it is also much easier to deposit a uniform film on a large area substrate [47]. Song and Lin observed that the hillock formation in a Pt/Ti film was obtained using UHV electron beam evaporation, but a rosette-type microstructure in the Pt/Ti film was obtained using DC-sputtering [48]. Aside from this, Zhou et al. indicated that the increased roughness improved the light scattering of the counter electrode [49].

Figure 6 shows the CVs of the Pt(E), Pt(S), Pt(E)/NiO, and Pt(S)/NiO counter electrodes. The oxidation and reduction peaks of I^-/I_3^- on these counter electrodes are similar. For example, their oxidation potential ranges from 0.4 V to 0.9 V, and the reduction potential ranges from 0.0 V to 0.5 V (Figure 6). The presence of a NiO film enhances the current density during the redox process. For example, in the oxidation process, the highest current density of Pt(E)/NiO (7.2 mA/cm^2) exceeds that of Pt(E) (6.1 mA/cm^2). In the reduction process, the lowest current density of Pt(E)/NiO (−5.2 mA/cm^2) also exceeds that of Pt(E) (−3.9 mA/cm^2). This result is attributed to the fact that a larger active surface area due to a deposited NiO film corresponds to a more energetic electrocatalytic activity. A similar tendency was also observed by Kim et al. [45] and Yoon et al. [46].

3.3. Photoelectrochemical Behaviour. The J-V characteristics of DSSC in all tests are shown in Figure 7, and Table 1 presents the open-circuit photovoltage (V_{oc}), the short-circuit photocurrent per unit area (J_{sc}), the fill factor (FF), and the power conversion efficiency (η) of the DSSC in tests D1 to D8. In this study, the V_{oc} of the DSSC is kept at 0.65 V. The power conversion efficiency of DSSC with Pt(E) (or Pt(E)/NiO) exceeds 3%.

At a fixed counter electrode, as the average thickness of TiO_2 film increases, the power conversion efficiency increases. For example, for the Pt(E) counter electrode, the power conversion efficiency increases from 3.00% to 3.16% as the average thickness of the TiO_2 film increases from 12.0 μm (in test D1) to 19.0 μm (in test D2). The J-V curve of DSSC with a thicker TiO_2 film is above that of DSSC with a thinner TiO_2 film (Figure 7). This result is due to the following: (1) a TiO_2 film with a larger average thickness contains more TiO_2 (P-25) particles, which may absorb more ultraviolet light; (2) the working electrode with a thicker TiO_2 film corresponds to a higher adsorptive capability of the dye because more tiny cavities are created in this film on a FTO-glass substrate so that the larger number of electrons may be excited as the DSSC is exposed to the light.

Although the average thickness of the TiO_2 film in test D1 (12.0 μm) is very close to that in test D3 (11.0 μm), the power conversion efficiency of DSSC with a Pt(E) counter electrode in test D1 (3.00%) substantially exceeds that of DSSC with a Pt(S) counter electrode in test D3 (2.33%). This result may be due to the following:. (1) the Pt(S) counter electrode sheet resistance (9.73 Ω/*sq*) significantly exceeds the Pt(E) counter electrode sheet resistance (5.57 Ω/sq); (2) at a fixed wavelength, the Pt(E) counter electrode reflectance remarkably exceeds the Pt(S) counter electrode reflectance. Fang et al. showed that in order for a DSSC to have better power conversion efficiency, a counter electrode should have the following characteristics: (1) good conductivity for transferring electrons, (2) excellent catalytic activity for I^-/I_3^- redox, and (3) light-reflecting ability to improve light-harvesting efficiency [50].

Most interestingly, the presence of a NiO film remarkably promotes the power conversion efficiency of DSSC. For example, the power conversion efficiencies of DSSC in tests D2 (with a Pt(E) counter electrode) and D6 (with a Pt(E)/NiO counter electrode) are 3.16% and 4.28%, respectively. Furthermore, the power conversion efficiencies of DSSC in tests D4 (with a Pt(S) counter electrode) and D8 (with a Pt(S)/NiO counter electrode) are 2.34% and 2.92%, respectively. These results are due to the following: (1) the

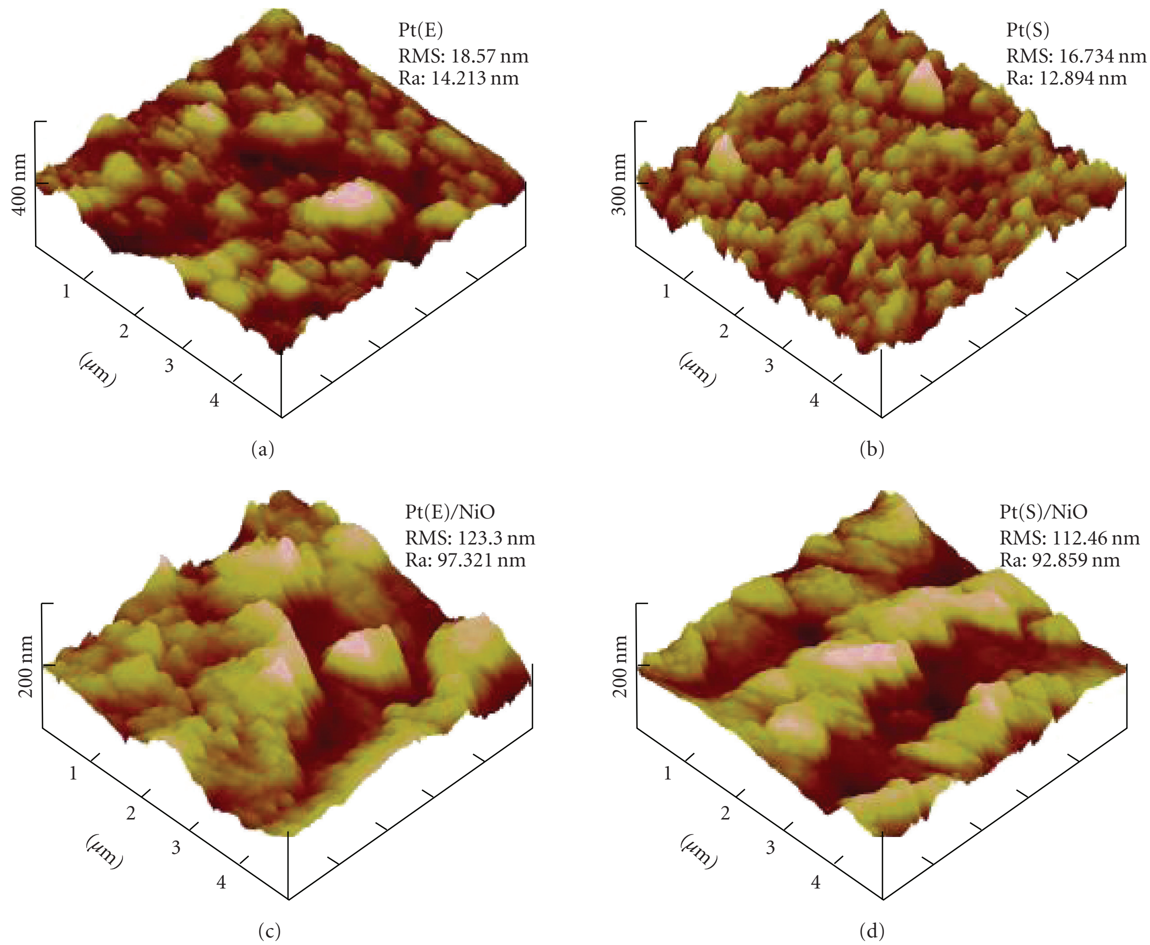

FIGURE 5: The 3-D micro-structure of counter electrodes. (a) Pt(E), (b) Pt(S), (c) Pt(E)/NiO, and (d) Pt(S)/NiO.

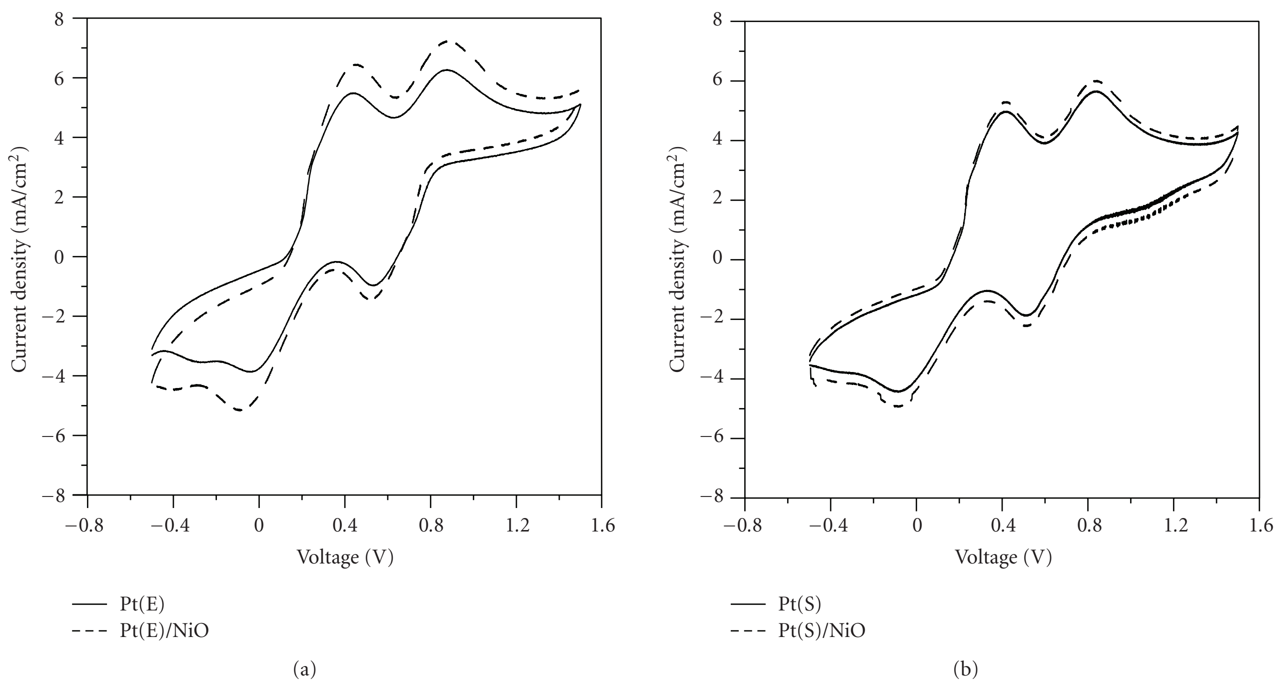

FIGURE 6: Cyclic voltammograms (CVs) of counter electrodes of Pt(E), Pt(S), Pt(E)/NiO, and Pt(S)/NiO.

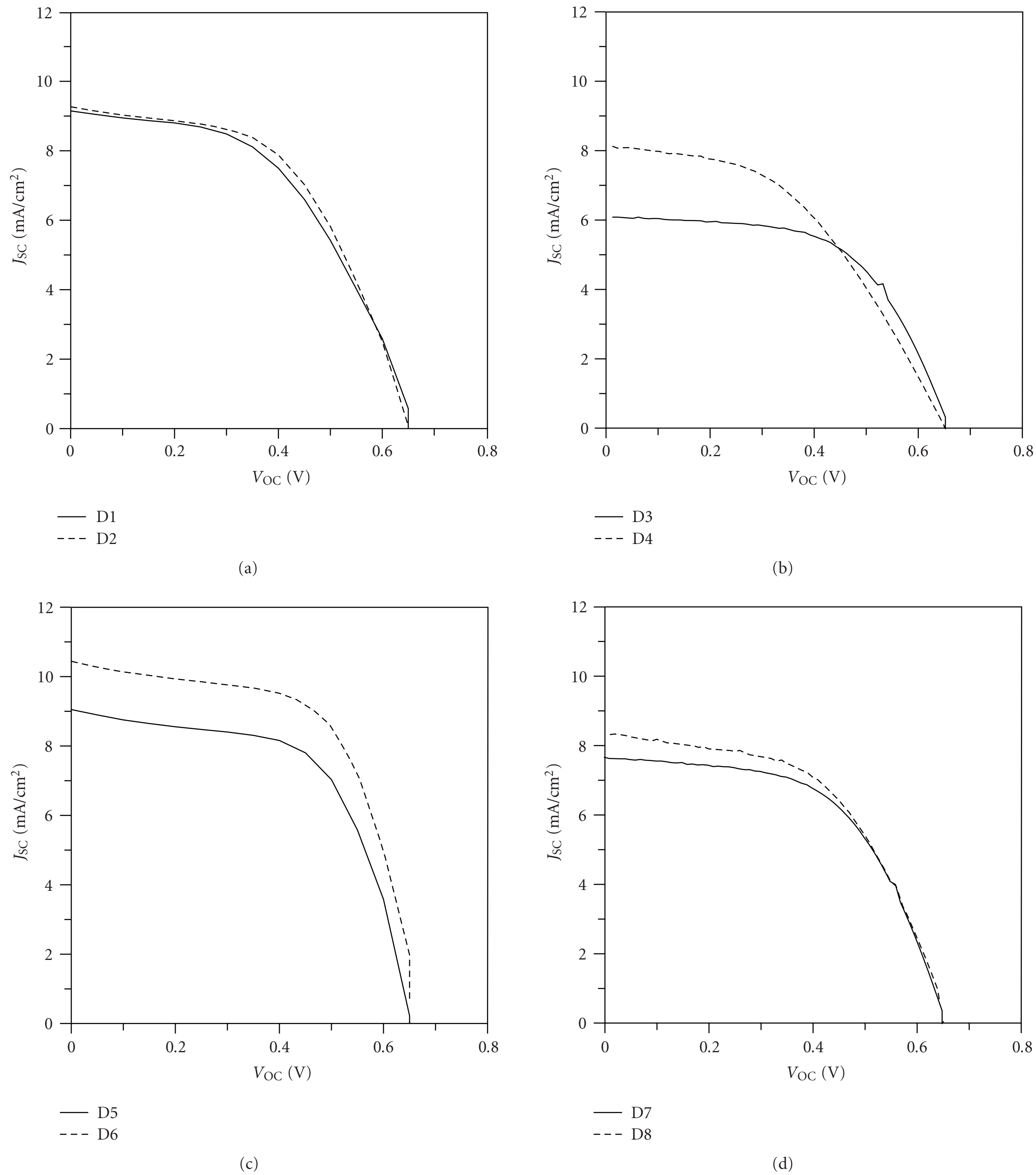

FIGURE 7: J-V characteristics in tests D1 to D8.

NiO film deposited on top of Pt(E) (or Pt(S)) substantially enhances the surface roughness average (Ra) of the counter electrode (Table 1); (2) the increased roughness improves the light scattering as well as the electroactive area of a counter electrode. Kim et al. [45] showed that the overall conversion efficiency of DSSC increased to 3.62% and 4.21% through the use of Pt/NiO and Pt/TiO_2 bi-phase counter electrodes, respectively.

4. Conclusion

The effect of different kinds of counter electrodes on the power conversion efficiency of a DSSC was investigated. The power conversion efficiency of the DSSC with a Pt(E) counter electrode exceeds that of the DSSC with a Pt(S) counter electrode because the Pt(E) counter electrode has better reflectance. Furthermore, the power conversion efficiency of the DSSC with a Pt(E)/NiO counter electrode exceeds that of the DSSC with a Pt(E) counter electrode because the Pt(E)/NiO counter electrode has better electrocatalytic activity. Most importantly, this study supports the application of a NiO film deposited on the Pt-FTO substrate using a simple spin coating method to improve the performance of a DSSC. However, the optimal process for fabricating a DSSC with a NiO film on the counter electrode, which can promote the electrocatalytic activity of the counter electrode, must be implemented to yield a DSSC with a satisfactory power conversion efficiency.

Concerning the possible application of this nontransparent cathode that the NiO is deposited on top of the Pt film, it may decline the transparency of photovoltaic windows. However, besides photovoltaic windows, the other real applications of DSSC, such as DSSC lampshade, flower-shaped DSSC, and leaf-shaped DSSC, whose transparency may not be seriously considered, have received substantial attention, too. We believe that this counter electrode may facilitate the performance of aforementioned devices of DSSC.

Acknowledgments

The authors would like to thank the National Science Council, Taiwan for financially supporting this research under Contract nos. NSC 97-2221-E-020-035 and NSC 97-2918-I-020-001. The authors would also like to thank the National Pingtung University of Science and Technology, Taiwan for their financial support to establish the Research Center of Solar Photo-Electricity Applications.

References

[1] B. O'Regan and M. Grätzel, "A low-cost, high-efficiency solar cell based on dye-sensitized colloidal TiO_2 films," *Nature*, vol. 353, no. 6346, pp. 737–740, 1991.

[2] N. S. Lewis, "Toward cost-effective solar energy use," *Science*, vol. 315, no. 5813, pp. 798–801, 2007.

[3] S. Kim, D. Kim, H. Choi et al., "Enhanced photovoltaic performance and long-term stability of quasi-solid-state dye-sensitized solar cells via molecular engineering," *Chemical Communications*, no. 40, pp. 4951–4953, 2008.

[4] M. Wei, Y. Konishi, H. Zhou, H. Sugihara, and H. Arakawa, "Utilization of titanate nanotubes as an electrode material in dye-sensitized solar cells," *Journal of the Electrochemical Society*, vol. 153, no. 6, pp. A1232–A1236, 2006.

[5] G.-S. Kim, H.-K. Seo, V. P. Godble, Y.-S. Kim, O.-B. Yang, and H.-S. Shin, "Electrophoretic deposition of titanate nanotubes from commercial titania nanoparticles: application to dye-sensitized solar cells," *Electrochemistry Communications*, vol. 8, no. 6, pp. 961–966, 2006.

[6] S.-J. Roh, R. S. Mane, S.-K. Min, W.-J. Lee, C. D. Lokhande, and S.-H. Han, "Achievement of 4.51% conversion efficiency using ZnO recombination barrier layer in TiO_2 based dye-sensitized solar cells," *Applied Physics Letters*, vol. 89, no. 25, Article ID 253512, 2006.

[7] Y. H. Su, W. H. Lai, L. G. Teoh, M. H. Hon, and J. L. Huang, "Layer-by-layer Au nanoparticles as a Schottky barrier in a water-based dye-sensitized solar cell," *Applied Physics A*, vol. 88, no. 1, pp. 173–178, 2007.

[8] J. Bandara and J. P. Yasomanee, "P-type oxide semiconductors as hole collectors in dye-sensitized solid-state solar cells," *Semiconductor Science and Technology*, vol. 22, no. 2, pp. 20–24, 2007.

[9] S. Ito, T. N. Murakami, P. Comte et al., "Fabrication of thin film dye sensitized solar cells with solar to electric power conversion efficiency over 10%," *Thin Solid Films*, vol. 516, no. 14, pp. 4613–4619, 2008.

[10] S. Sumikura, S. Mori, S. Shimizu, H. Usami, and E. Suzuki, "Syntheses of NiO nanoporous films using nonionic triblock co-polymer templates and their application to photo-cathodes of p-type dye-sensitized solar cells," *Journal of Photochemistry and Photobiology A*, vol. 199, no. 1, pp. 1–7, 2008.

[11] S. Sumikura, S. Mori, S. Shimizu, H. Usami, and E. Suzuki, "Photoelectrochemical characteristics of cells with dyed and undyed nanoporous p-type semiconductor CuO electrodes," *Journal of Photochemistry and Photobiology A*, vol. 194, no. 2-3, pp. 143–147, 2008.

[12] C.-S. Chou, R.-Y. Yang, M.-H. Weng, and C.-H. Yeh, "Study of the applicability of TiO_2/dye composite particles for a dye-sensitized solar cell," *Advanced Powder Technology*, vol. 19, no. 6, pp. 541–558, 2008.

[13] C.-S. Chou, R.-Y. Yang, M.-H. Weng, and C.-H. Yeh, "Preparation of TiO_2/dye composite particles and their applications in dye-sensitized solar cell," *Powder Technology*, vol. 187, no. 2, pp. 181–189, 2008.

[14] K.-M. Lee, C.-W. Hu, H.-W. Chen, and K.-C. Ho, "Incorporating carbon nanotube in a low-temperature fabrication process for dye-sensitized TiO_2 solar cells," *Solar Energy Materials and Solar Cells*, vol. 92, no. 12, pp. 1628–1633, 2008.

[15] B. Yoo, K. Kim, S. H. Lee, W. M. Kim, and N.-G. Park, "ITO/ATO/TiO_2 triple-layered transparent conducting substrates for dye-sensitized solar cells," *Solar Energy Materials and Solar Cells*, vol. 92, no. 8, pp. 873–877, 2008.

[16] B. N. Pawar, G. Cai, D. Ham et al., "Preparation of transparent and conducting boron-doped ZnO electrode for its application in dye-sensitized solar cells," *Solar Energy Materials and Solar Cells*, vol. 93, no. 4, pp. 524–527, 2009.

[17] K.-M. Lee, V. Suryanarayanan, and K.-C. Ho, "Influences of different TiO_2 morphologies and solvents on the photovoltaic performance of dye-sensitized solar cells," *Journal of Power Sources*, vol. 188, no. 2, pp. 635–641, 2009.

[18] W. J. Lee, E. Ramasamy, and D. Y. Lee, "Effect of electrode geometry on the photovoltaic performance of dye-sensitized solar cells," *Solar Energy Materials and Solar Cells*, vol. 93, no. 8, pp. 1448–1451, 2009.

[19] U. O. Krašovec, M. Berginc, M. Hočevar, and M. Topič, "Unique TiO_2 paste for high efficiency dye-sensitized solar cells," *Solar Energy Materials and Solar Cells*, vol. 93, no. 3, pp. 379–381, 2009.

[20] T. Sawatsuk, A. Chindaduang, C. Sae-kung, S. Pratontep, and G. Tumcharern, "Dye-sensitized solar cells based on TiO_2-MWCNTs composite electrodes: performance improvement and their mechanisms," *Diamond and Related Materials*, vol. 18, no. 2-3, pp. 524–527, 2009.

[21] H. Wang, Y. Liu, H. Xu et al., "An investigation on the novel structure of dye-sensitized solar cell with integrated photoanode," *Renewable Energy*, vol. 34, no. 6, pp. 1635–1638, 2009.

[22] C.-S. Chou, R.-Y. Yang, C.-K. Yeh, and Y.-J. Lin, "Preparation of TiO_2/Nano-metal composite particles and their applications in dye-sensitized solar cells," *Powder Technology*, vol. 194, no. 1-2, pp. 95–105, 2009.

[23] S. Hwang, J. H. Lee, C. Park et al., "A highly efficient organic sensitizer for dye-sensitized solar cells," *Chemical Communications*, no. 46, pp. 4887–4889, 2007.

[24] J.-G. Chen, C.-Y. Chen, S.-J. Wu, J.-Y. Li, C.-G. Wu, and K.-C. Ho, "On the photophysical and electrochemical studies of dye-sensitized solar cells with the new dye CYC-B1," *Solar Energy Materials and Solar Cells*, vol. 92, no. 12, pp. 1723–1727, 2008.

[25] S. Ito, H. Miura, S. Uchida et al., "High-conversion-efficiency organic dye-sensitized solar cells with a novel indoline dye," *Chemical Communications*, no. 41, pp. 5194–5196, 2008.

[26] M. Xu, R. Li, N. Pootrakulchote et al., "Energy-level and molecular engineering of organic D-π-A sensitizers in dye-sensitized solar cells," *Journal of Physical Chemistry C*, vol. 112, no. 49, pp. 19770–19776, 2008.

[27] C.-H. Yang, H.-L. Chen, Y.-Y. Chuang et al., "Characteristics of triphenylamine-based dyes with multiple acceptors in application of dye-sensitized solar cells," *Journal of Power Sources*, vol. 188, no. 2, pp. 627–634, 2009.

[28] J. Pei, S. Peng, J. Shi et al., "Triphenylamine-based organic dye containing the diphenylvinyl and rhodanine-3-acetic acid moieties for efficient dye-sensitized solar cells," *Journal of Power Sources*, vol. 187, no. 2, pp. 620–626, 2009.

[29] V. Kandavelu, H.-S. Huang, J.-L. Jian, T. C.-K. Yang, K.-L. Wang, and S.-T. Huang, "Novel iminocoumarin dyes as photosensitizers for dye-sensitized solar cell," *Solar Energy*, vol. 83, no. 4, pp. 574–581, 2009.

[30] T. Kato, T. Kado, S. Tanaka, A. Okazaki, and S. Hayase, "Quasi-solid dye-sensitized solar cells containing nanoparticles modified with ionic liquid-type molecules," *Journal of the Electrochemical Society*, vol. 153, no. 3, pp. A626–A630, 2006.

[31] T. C. Wei, C. C. Wan, and Y. Y. Wang, "Preparation and characterization of a micro-porous polymer electrolyte with cross-linking network structure for dye-sensitized solar cell," *Solar Energy Materials and Solar Cells*, vol. 91, no. 20, pp. 1892–1897, 2007.

[32] S. Ganesan, B. Muthuraaman, V. Mathew, J. Madhavan, P. Maruthamuthu, and S. Austin Suthanthiraraj, "Performance of a new polymer electrolyte incorporated with diphenylamine in nanocrystalline dye-sensitized solar cell," *Solar Energy Materials and Solar Cells*, vol. 92, no. 12, pp. 1718–1722, 2008.

[33] Y. Wang, Y. Sun, B. Song, and J. Xi, "Ionic liquid electrolytes based on 1-vinyl-3-alkylimidazolium iodides for dye-sensitized solar cells," *Solar Energy Materials and Solar Cells*, vol. 92, no. 6, pp. 660–666, 2008.

[34] D. Shi, N. Pootrakulchote, R. Li et al., "New efficiency records for stable dye-sensitized solar cells with low-volatility and ionic liquid electrolytes," *Journal of Physical Chemistry C*, vol. 112, no. 44, pp. 17046–17050, 2008.

[35] K.-M. Lee, P.-Y. Chen, C.-P. Lee, and K.-C. Ho, "Binary room-temperature ionic liquids based electrolytes solidified with SiO_2 nanoparticles for dye-sensitized solar cells," *Journal of Power Sources*, vol. 190, no. 2, pp. 573–577, 2009.

[36] T. Kato and S. Hayase, "Quasi-solid dye sensitized solar cell with straight ion paths. Proposal of hybrid electrolytes for ionic liquid-type electrolytes," *Journal of the Electrochemical Society*, vol. 154, no. 1, pp. B117–B121, 2007.

[37] A. Kay and M. Grätzel, "Low cost photovoltaic modules based on dye sensitized nanocrystalline titanium dioxide and carbon powder," *Solar Energy Materials and Solar Cells*, vol. 44, no. 1, pp. 99–117, 1996.

[38] T. N. Murakami, S. Ito, Q. Wang et al., "Highly efficient dye-sensitized solar cells based on carbon black counter electrodes," *Journal of the Electrochemical Society*, vol. 153, no. 12, pp. A2255–A2261, 2006.

[39] Z. Huang, X. Liu, K. Li et al., "Application of carbon materials as counter electrodes of dye-sensitized solar cells," *Electrochemistry Communications*, vol. 9, no. 4, pp. 596–598, 2007.

[40] C.-S. Chou, R.-Y. Yang, M.-H. Weng, and C.-I. Huang, "The applicability of SWCNT on the counter electrode for the dye-sensitized solar cell," *Advanced Powder Technology*, vol. 20, no. 4, pp. 310–317, 2009.

[41] E. Ramasamy, W. J. Lee, D. Y. Lee, and J. S. Song, "Spray coated multi-wall carbon nanotube counter electrode for tri-iodide (I_3^-) reduction in dye-sensitized solar cells," *Electrochemistry Communications*, vol. 10, no. 7, pp. 1087–1089, 2008.

[42] E. Ramasamy, W. J. Lee, D. Y. Lee, and J. S. Song, "Nanocarbon counterelectrode for dye sensitized solar cells," *Applied Physics Letters*, vol. 90, no. 17, Article ID 173103, 2007.

[43] W. J. Lee, E. Ramasamy, D. Y. Lee, and J. S. Song, "Grid type dye-sensitized solar cell module with carbon counter electrode," *Journal of Photochemistry and Photobiology A*, vol. 194, no. 1, pp. 27–30, 2008.

[44] S.-S. Kim, K.-W. Park, J.-H. Yum, and Y.-E. Sung, "Pt-NiO nanophase electrodes for dye-sensitized solar cells," *Solar Energy Materials and Solar Cells*, vol. 90, no. 3, pp. 283–290, 2006.

[45] S.-S. Kim, K.-W. Park, J.-H. Yum, and Y.-E. Sung, "Dye-sensitized solar cells with Pt-NiO and Pt-TiO_2 biphase counter electrodes," *Journal of Photochemistry and Photobiology A*, vol. 189, no. 2-3, pp. 301–306, 2007.

[46] C. H. Yoon, R. Vittal, J. Lee, W.-S. Chae, and K.-J. Kim, "Enhanced performance of a dye-sensitized solar cell with an electrodeposited-platinum counter electrode," *Electrochimica Acta*, vol. 53, no. 6, pp. 2890–2896, 2008.

[47] H. Fornander, J. Birch, P. Sandström, and J.-E. Sundgren, "Structure evolution of epitaxial Pd grown on MgO(001): a comparison between sputtering and electron-beam evaporation," *Thin Solid Films*, vol. 349, no. 1, pp. 4–9, 1999.

[48] Z. Song and C. Lin, "Microstructure and electrical properties of $PbZr_{0.48}Ti_{0.52}O_3$ ferroelectric films on different Pt bottom electrodes," *Applied Surface Science*, vol. 158, no. 1, pp. 21–27, 2000.

[49] K. Imoto, K. Takahashi, T. Yamaguchi, T. Komura, J.-I. Nakamura, and K. Murata, "High-performance carbon counter electrode for dye-sensitized solar cells," *Solar Energy Materials and Solar Cells*, vol. 79, no. 4, pp. 459–469, 2003.

[50] X. Fang, T. Ma, G. Guan, M. Akiyama, T. Kida, and E. Abe, "Effect of the thickness of the Pt film coated on a counter electrode on the performance of a dye-sensitized solar cell," *Journal of Electroanalytical Chemistry*, vol. 570, no. 2, pp. 257–263, 2004.